M4B: A Tool for the Multiphysics Analysis of the Deformational Behaviour of Soils and its Interaction with Building Foundations

J. Alonso[*1], M. Moya[1] J. González[1], L. Asensio[1] and V. Navarro[1]
[1]Geoenvironmental Engineering Group. Universidad de Castilla-La Mancha.
*Corresponding author: Juan Alonso. Escuela de Arquitectura de Toledo. Campus de la Fábrica de Armas, juan.alonso@uclm.es

Abstract: The Geoenvironmental Engineering Group of the University of Castilla-La Mancha, Spain, is developing a computational tool, M4B, for describing the influence of environmental loads on the deformational behavior of soils and its interaction with building foundations. This tool comprises a set of algorithmic files in text format which can be implemented in Comsol Multiphysics® by using the Multiphysics node. There are two different kind of files: databases and function files. Databases include an extensive relation of reaction rates and thermodynamic parameters for the prediction of dissolution and precipitation of mineral phases. Function files include hydraulic and mechanical constitutive models, with some innovative numerical strategies for the prediction of stress-strain behavior under elastic-plastic paths. To illustrate the M4B scope, the simulation of an excavation (considering short and long term behavior under a changing hydro-thermal-mechanical and chemical environment) is shown in this work.

Keywords: Soil-structure interaction, coupled geomechanics problems.

1. Introduction

The prediction of soil behaviour and its interaction with building structures should deal, in some circumstances, with complex physical and chemical coupled processes, such as dissecation due to evaporation, volume changes related to suction variations, dissolution or precipitation of mineral phases, or changes in the chemical activity. Some of these issues can be solved with computer programs that are available for the modelling of coupled multiphysics problems. The main problem related with some of these programs is the limited accessibility to the equations for the user. In some other cases, such as with "in house" developed software, the modification or introduction of new equations can become a very difficult issue due to the long time needed for their development, instead of their versatility.

The use of a multiphysics solver such as Comsol Multiphysics (CM) facilitates the development of numerical models involving several processes due to its great flexibility in the implementation of equations formulated by the user. The performance of this computer program can be greatly extended by the user through the definition of the equations needed for the solution of an specific problem. This paper describes the equations included in M4B, a tool containing a series of algorithmic files with the definition of the equations for the solving of complex geotechnical problems involving multiphysics couplings and running under CM environment. Furthermore, an example problem is presented where M4B is used.

2. Equations contained in M4B databases

2.1 Hydraulic Equations

The water content condition is characterized by solving the water mass balance equation:

$$[1] \qquad \frac{D_S m^W}{Dt} + m^W \nabla \cdot \boldsymbol{v}_s + \nabla \cdot (\rho^W \boldsymbol{q}^W) = 0$$

where $\boldsymbol{v}_S$ is the velocity of the solid skeleton, and m^W, ρ^W y $\boldsymbol{q}^W$ are the mass of water per unit volume, the density, and the water flux, respectively. D/D_t is the material time derivative. The mass of water is defined as[2:

$$[2] \qquad m^W = n S_L \rho_L^W + n S_G \rho_G^W$$

being n the porosity, and ρ_L^W and ρ_G^W the densities of water in liquid and gaseous phase, respectively. S_L is the liquid degree of saturation, and S_G is the gas one, being S_G =1- S_L. S_L is obtained as function of matric suction by a

retention curve, that must be obtained experimentally for each type of material. Brooks and Corey [1] or van Genuchten [2] models are included in M4B.

The mass water flux is defined as:

[3]

$$\rho^W \boldsymbol{q}^W = -\rho_L^{\mathrm{W}} \frac{\boldsymbol{K}_L k_{rL}^{\mathrm{W}}}{\mu_L} (\nabla P_L + \rho g \nabla z) - n\ \tau D_v \nabla \cdot \rho_G^{\mathrm{W}}$$

where the first term in right hand side describes the advective flux of water, obtained by Darcy´s law. $\boldsymbol{K}_{\mathrm{L}}$, μ_{L}, P_{L} y ρ_{L} are intrinsic permeability, dynamic viscosity, liquid pressure and average density of the phase, respectively. $k_{\mathrm{rL}}{}^{\mathrm{k}}$ is the relative permeability, and ∇_z is the gradient related to the vertical coordinate, z. The second term describes de dispersive flux of water vapour. This flux is defined by Fick´s law, D_{V} being the efective coeficient of molecular diffusion in a porous medium, a function of temperature, gas pressure, tortuosity and degree of saturation. The density of water vapour is obtained as:

[4] $$\rho_G^{\mathrm{W}} = \frac{W_W P_V}{RT}$$

being W_{W} the molecular weight of water, R is the universal constant for ideal gases, T is the temperature and P_{v} is the vapour pressure. It can be obtained as [3]:

[5] $$P_V = HP_V^0$$

H being the relative vapour pressure, and P_V^0 the equilibrium vapour pressure with free water, which is exclusively dependent on temperature. The relative vapour pressure is obtained from:

[6] $$H = \exp\left[\frac{W_W s}{\rho_L RT}\right]$$

where s is the matric suction, defined as the difference between liquid and gas pressure (s=P_{L}-P_{G}). If gas pressure is considered as constant, suction changes are only related to liquid pressure variations.

2.2 Thermal Equations

The temperature field is solved by the energy conservation equation:

[7] $$\frac{\partial}{\partial t}[E] + \nabla(\boldsymbol{l}_E) = f^Q$$

E being the internal energy of the material, $\boldsymbol{l}_{\mathrm{E}}$ the heat flux, f^Q the source/sink term. The internal energy of the porous media is the sum of the internal energies of each phase, solid E_{S}, liquid E_{L} and gas E_{G}:

[8] $$E = E_S + E_L + E_G$$

[9] $$E_S = c_S \rho_S (1-n) T$$

[10] $$E_L = c_L^W \rho_L^W S_L n\ T$$

[11] $$E_G = c_G^W \rho_G^W S_G nT + l\rho_G^W S_G n$$

where c_i^j is the specific heat of the component j in phase i and l is the latent heat of evaporation/condensation. The heat flux is composed of the fluxes of the different phases, plus an advective component:

[12] $$\boldsymbol{l}_E = \boldsymbol{i}_C + \boldsymbol{l}_S + \boldsymbol{l}_L + \boldsymbol{l}_G$$

The conduction heat flux is governed by Fourier´s Law:

[13] $$\boldsymbol{i}_C = -\lambda(\boldsymbol{T}) \nabla T$$

being λ the thermal conductivity. In a multiphysics medium, this value can be obtained as an averaged contribution of the different phases as:

[14] $$\lambda = \lambda_S^{1-n} \lambda_L^{S_L n} \lambda_G^{(1-S_L)n}$$

The following equations are used to define the advective components of heat flux related to soil, liquid and gas movement:

[7] $$\boldsymbol{l}_S = E_S \rho_S (1-n) \boldsymbol{v}_s$$

[16] $$\boldsymbol{l}_L = \boldsymbol{q}_L^W E_L + E_L \boldsymbol{v}_s$$

[17] $$\boldsymbol{l}_G = \boldsymbol{q}_G^W E_G + E_G \boldsymbol{v}_s$$

2.3 Chemical Equations

The following equations define the mass balance of each chemical species:

[18] $$\frac{\partial n S_L C_i}{\partial t} + \nabla \boldsymbol{j}_i = n S_L (R_i + R_i^{MIN})$$
$$\frac{\partial m_{MIN,i}}{\partial t} = -m_{MIN,i} \nabla \cdot \boldsymbol{v}_s + R_i^{MIN}$$

where C_i is the concentration of the species, $m_{MIN,i}$ the amount of precipitated material, R_i y R_i^{MIN} are the net production rates of chemical species i as a consequence of chemical reactions and sorption or precipitation/dissolution processes, respectively. The resolution of these equations implies a high computational effort due to the different rates between the fluxes and reaction rates involved. For this reason, and with the aim of reducing the number of equations involved, the equations were rewritten in terms of conserved quantities, following a similar procedure as used by Jacobs and Probstein [4]. This approach results in equations where reaction rate components are neglected, excluding those for the calculation of adsorption or precipitation processes. The total amount of a conserved quantity is obtained from:

[8] $$T_k = \sum_{i=1}^{N} \alpha_{ik} \left(C_i + C_i^a \right) \qquad \forall k = 1,...,M$$

where T_K defines the total amount of each conserved substance, α_{ik} states the contribution of each species i to the conserved substance K, N is the number of species and M is the number of conserved substances considered. Combining Eqs. 18 and 19 the following equation remains:

[20] $$\sum_{i=1}^{N} \alpha_{ik} \left(\frac{\partial n S_L \left(C_i + C_i^a \right)}{\partial t} + \nabla \boldsymbol{j}_i = n S_L R_i \right) = 0$$
$$k = 1,..., M$$

And since the total mass of each substance is preserved, we would have:

[21] $$\sum_{i=1}^{N} \alpha_{ik} R_i = 0$$

The following equation for each conserved substance quantity is obtained:

[22] $$\frac{\partial n S_L T_k}{\partial t} + \sum_{i=1}^{N} \alpha_{ik} \nabla \boldsymbol{j}_i = 0 \quad k = 1,...,M$$

The equations for the species shown in table 1 were included in M4B.

Table 1: Primary and Secondary species considered in M4B databases

CONSERVED SUBSTANCES	H^+, CO_3^{2-}, SO_4^{2-}, Ca^{2+}, Mg^{2+}, Na^+, K^+, Cl^-
SPECIES	HCO_3^-, OH^-, H_2CO_3, HSO_4^-, H_2SO_4, $CaHCO_3^+$, $CaCO_3$, $CaHSO_4^+$, $CaSO_4$, $CaOH^+$, $MgHCO_3^+$, $MgCO_3$, $MgSO_4$, $MgOH^+$, $NaHCO_3$, $NaCO_3^-$, $NaSO_4^-$, $NaOH$, KOH, H^+, CO_3^{2-}, SO_4^{2-}, Ca^{2+}, Mg^{2+}, Na^+, K^+, Cl^-

The concentration of the different species are calculated from equilibrium constants. If the principle of electroneutrality is taken into account, one of the conservation equations can be eliminated:

[23] $$\sum_{i=1}^{N} z_i C_i = 0$$

The molar flux of species per unit area, is given by the contribution of an advective and a diffusive component, as shown in the following expression:

[24] $$\boldsymbol{j}_i = \boldsymbol{q}^W C_i - n S_L D_i \nabla C_i$$

2.4 Mechanical Equations

Mechanical behavior modeling is based on the resolution of the equilibrium equation, which can be expressed as:

[9] $$\nabla \boldsymbol{\sigma}_{TOT} + \rho g \nabla z = 0$$

This equation is implemented in the basic module of CM with a series of mechanical elementary constitutive models, and its resolution gives the field of displacements, which are the variables to be determined during the calculation process, as well as the stress and strain fields.

For the definition of the mechanical constitutive behaviour, the following constitutive stresses, $\boldsymbol{\sigma}$, are proposed:

$$[26] \qquad \boldsymbol{\sigma} = \boldsymbol{\sigma}_{\mathrm{TOT}} - P_{\phi}\boldsymbol{m}$$

being m the vector expression of the Kronecker delta and P_{ϕ} the pore pressure, which adopts the maximum value among the liquid and the gas pressure:

$$[27] \qquad P_{\phi} = \max(P_{\mathrm{G}}, P_{\mathrm{L}})$$

By this definition, the constitutive stress has the meaning of the effective stress if a full saturation is developed, and of the net stress in case of a partially saturated medium. In the generalized formulation adopted in M4B the variation of the constitutive stresses is obtained from the following expression:

$$[28] \qquad d\boldsymbol{\sigma} = \boldsymbol{D}^{el}\left(d\boldsymbol{\varepsilon} - d\boldsymbol{\varepsilon}^{s} - d\boldsymbol{\varepsilon}^{CH} - d\boldsymbol{\varepsilon}^{m} - d\boldsymbol{\varepsilon}^{p}\right)$$

being $d\boldsymbol{\varepsilon}$ the incremental strain, $\boldsymbol{D}^{\mathrm{el}}$ the elastic matrix associated to mechanical loading, and the rest of the terms of the equation are the components of strain not associated with the mechanical strain: strain variations due to suction $d\boldsymbol{\varepsilon}^{\mathrm{S}}$, precipitation or dissolution of minerals $d\boldsymbol{\varepsilon}^{\mathrm{CH}}$, volumetric changes of the microstructure $d\boldsymbol{\varepsilon}^{\mathrm{m}}$, and plastic deformations $d\boldsymbol{\varepsilon}^{\mathrm{P}}$.

The rate of plastic and microstructure strains depends on the constitutive model adopted. M4B includes some basic constitutive mechanical models defined through state surfaces. Furthermore, some more complex mechanical elastic-plastic constitutive models for soils, including critical state models, and others that take into account microstructure changes, are also available and were implemented in CM for the modeling of some complex coupled problems involving multiphysics interactions (see [5-7], for example).

The elastic strain component related to suction is given by the following expression:

$$[29] \qquad d\boldsymbol{\varepsilon}^{s} = \frac{\boldsymbol{\kappa}_{S}}{(s + P_{atm})}\, ds$$

where κ_{S} is the soil stiffness to suction changes.

The increase in deformation component associated with mineral precipitation or dissolution can be defined through the following expression, modified form Oldecop and Alonso [8]:

$$[10] \qquad d\boldsymbol{\varepsilon}_{V}^{CH} = \sum_{i} \frac{\gamma_{i}}{\rho_{i}} W_{\mathrm{i}} R_{i}^{MIN}$$

where W_{i} is the molecular weight of the precipitated mineral and γ_{i} is a coefficient measuring the bulking effect induced by crystal growth in the rock mass. Dissolution or precipitation rate for each mineral is given by the following expression, modified from Lasaga [9]:

$$[11] \qquad R_{i}^{MIN} = \frac{1}{W_{\mathrm{i}}} \sigma_{c} k \xi_{i} \phi_{i} \left\{ \left| \frac{IAP_{i}}{K_{i}} \right|^{\theta} - 1 \right\}^{n}$$

where IAP_i and K_i are the ionic activity product and the solubility product for each mineral reaction, respectively. The mineral phases considered, and their respective solubility products were obtained from databases shown in [10] and [11]. θ and n are constant parameters, σ_{c} is the specific surface of the precipitated mineral, k is a constant rate that controls the dissolution/precipitation rate, ϕ_{i} is the volumetric fraction of each mineral, and ξ_{i} is the sign for dissolution/precipitation. Finally, the definition of the variation of the total porosity, n, as a result of the precipitation or dissolution of minerals, can be expressed as:

$$[12] \qquad \frac{D_{S} n}{Dt} = (1 - n)\nabla \cdot \boldsymbol{v}_{s} - \sum_{i} \frac{1}{\rho_{i}} W_{\mathrm{i}} R_{i}^{MIN}$$

3. Implementation of M4B in COMSOL Multiphysics®

The equations for the definition of the hydraulic, thermal and chemical model are introduced in CM as PDE, general form, equations. The variables needed for the complete definition are compiled in a series of text files, which can be activated or deactivated depending on the study problem.

The mechanical behavior is formulated with the aid of the structural mechanics module available in CM. Nevertheless, because CM does not allow the introduction of implicit expressions between state functions, needed for the definition of some elastic-plastic constitutive models, some auxiliary equations are necessary to define changes in the stress state, the void ratio and the plastic variables used in the constitutive model. These equations are solved as ordinary differential equations (ODEs), through the temporary integration of variables with respect to incremental displacements, and simultaneously with the rest of equations [12]. For the modeling of the structural elements of the foundation, beam elements, available in the "Structural Mechanics Module" of CM, are used. This approach reduces significatively the computational cost and allows to easily obtain the internal forces of the structural elements. All these equations are fully coupled solved using CM capabilites.

4. Modelling of an excavation process

To show the scope of M4B for CM, the analysis of an excavation process and the subsequent change in the chemical environment due to the breaking of a pipe is shown for a clayey soil with low permeability and high concentration of sulfate in groundwater.

For predicting these processes in a particular emplacement, the equations described above were used. In the study case analyzed, an excavation of 10 m was considered. The geometry and mesh are show in figure 1. The detailed area shows the location of the pipe, with 1 m diameter, which goes underneath the excavation. The ground filling the trench of the pipe was assumed to be the same as the surrounding terrain, and completely consolidated. Geomechanical and hydraulic parameters are shown in table 2.

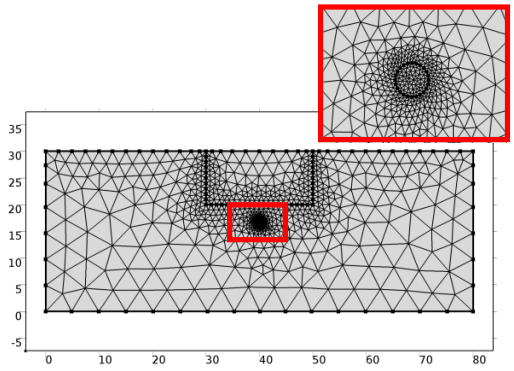

Figure 1. Domain geometry and mesh.

The model was performed through successive study steps. In the first step, a geostatic condition was achieved, where the stresses and pore pressures were obtained prior to excavation. The hydraulic boundary conditions imposed an initial water flux from right to left.

In the second study step, the excavation process was simulated. The pore pressure and stress distribution obtained in the first study step were used as the initial values of this study step, although the initial displacements were set to zero. The excavation was simulated by progressively reducing the gravitational forces, the elastic modulus and the permeability of the excavated volume. The excavation process produced a reduction in the pore pressure, as a consequence of the reduction of the total stresses due to the excavation, which changes the water flux in the system. This is shown in figure 2, where the vectors show the water flux in the system, pointing mainly to the bottom of the excavation. Pore pressure variations take place in an inverse consolidation process with a velocity that will depend on the permeability of the soil and the hydraulic boundary conditions. This process results in a heave at the bottom of the excavation, as shown in figure 3.

In the third study step, the structural elements (slab and walls) were built, and a change in the chemistry of the system was produced due to the fracture in the pipe beneath the excavation bottom. The water inside the pipe was assumed to be at the same pressure as the surrounding groundwater, and clear, with a low sulphate

concentration. This process was evaluated along 25 years time.

Table 2: Parameters used in the analysis

Parameter	Value
ρ_s , soil density	2650 kgm^{-3}
k_s, bulk modulus related to suction changes	-0.02 MPa^{-1}
γ, coefficient related to crystal growth pressure	1
Elastic modulus	17 MPa
Poisson coefficient	0.3
Initial porosity, n	0.4
Intrinsic permeability, $\boldsymbol{K}_L$	1.00 x 10^{-17} m^2
Initial gypsum content	20 %
Initial sulphate concentration	0.002 mol l^{-1}
Initial calcium concentration	0.014 mol l^{-1}
$k\sigma_c$	3.4 x 10^{-04} $kgm^{-2}s^{-1}$

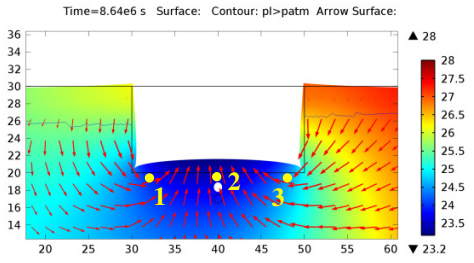

Figure 2. Water fluxes at the end of the excavation process (arrows). Contours show piezometric level values. Yellow dots show the place for displacement evaluation.

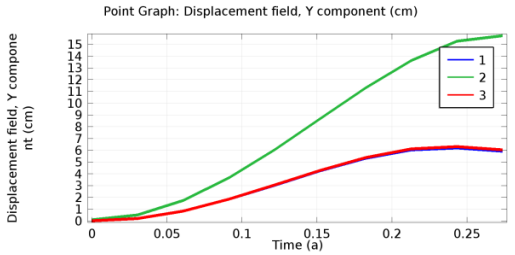

Figure 3. Heave produced during excavation study step at points 1, 2 and 3 (shown in figure 2). Heave at point 1 and 3 are overlapped.

The change on water chemistry, which was previously in equilibrium, produced a disturbance by undersaturation on the calcium sulphate around the pipe, triggering the dissolution of gypsum. This process resulted in a porosity increase (Fig. 4), and the development of settlement displacements (Figs. 5 and 6) due to changes in the resulting volumetric strains.

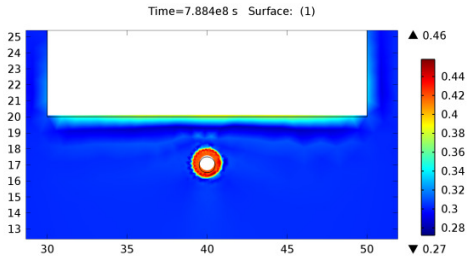

Figure 4. Porosity at the end of the of the third study step.

The resulting strains produced a modification in the internal forces of the beam elements considered in the model over time, as shown in figure 7.

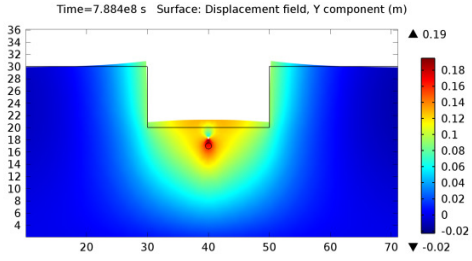

Figure 5. Displacement field at the end of the third study step.

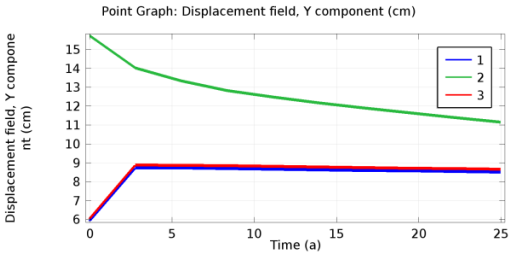

Figure 6. Settlement produced during the third study step at points 1, 2 and 3 (shown in figure 2).

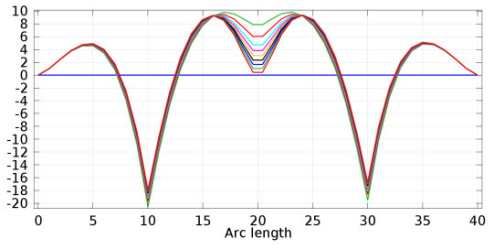

Figure 7. Evolution of the bending moments (kNm) obtained as a consequence of the gypsum dissolution beneath the excavation bottom.

5. Discussion and Conclussions

In the example analyzed, the excavation process introduced major changes to the initial state of the ground. On one hand, the terrain deconfinement caused a negative consolidation process, where the reduction of the gravitational forces occurred simultaneously to a decrease in the fluid pressure, and the development of heave displacements along a time subjected to permeability and the hydraulic boundary conditions. On the other hand, the dissolution of gypsum induced an increase on the porosity, and volumetric changes leading to settlement displacements. The model allows to determinate if damage is expected to occur in the structural elements due to the deformation history related to these processes.

This example shows that M4B for CM provides of several resources for the complete analysis of the coupled thermo-hydraulic-chemical-mechanical THCM behavior of soils and their interaction with building structures

6. References

1. Brooks RH and Corey AT. Hydraulic properties of porous media. Colorado State Univ. *Hydrology Paper* **3**, 27 pp (1964).
2. Van Genuchten, MT. A Closed-form equation for predicting the hydraulic conductivity of unsaturated soils. *Soil Sci. Soc. Am. J.* **44**, 892-898 (1980).
3. Pollock DW. Simulation of fluid flow and energy transport processes associated with high-level radioactive waste disposal in unsaturated alluvium, *Water resources research*, **22(5)**, 765-775 (1986).
4. Jacobs RA and Probstein RF. Two-Dimensional Modeling of *AIChE Journal* **42(6)**, 1685-1696 (1996).
5. Alonso J, Navarro V, Calvo B, Asensio L. Hydro-mechanical analysis of CO_2 storage in porous rocks using a critical state model. *Int. J. Rock Mech. Mining Sci.*, **54**, 19-26 (2012).
6. Navarro V, Asensio L, De la Morena G, Pintado X, Yustres A. Differentiated intra- and inter-aggregate water content models of mx-80 bentonite. *Applied Clay Science*, **118**, 325–336 (2015).
7. Navarro V, Asensio L, Yustres A, Pintado X, Alonso J. An elastoplastic model of bentonite free swelling, *Engineering Geology*, **181**,190–201 (2014).
8. Oldecop L and Alonso E. Modelling the degradation and swelling of clayey rocks bearing calcium-sulphate, *Int. J. Rock Mech. Mining Sci* **54**, 90–102 (2012).
9. Lasaga AC. Chemical kinetics of water-rock interactions, *J. Geophys. Res*. **89,** No. B6, 4009-4025 (1984).
10. ANDRA. https://www.thermochimie-tdb.com/pages/kinetic_models.php (2015).
11. Delany JM and Lundeen SR. The LLNL Thermochemical Database: Livermore, California, Lawrence Livermore National Laboratory Report UCRL-21658, 150 (1989).
12. Navarro V, Asensio L, Alonso J, Yustres A. Pintado, X. Multiphysics implementation of advanced soil mechanics models, *Computers and Geotechnics,* **60**, 20-28 (2014).